IEEE Access
Multidisciplinary | Rapid Review | Open Access Journal

Received December 8, 2021, accepted December 23, 2021, date of publication December 30, 2021,
date of current version January 7, 2022.

Digital Object Identifier 10.1109/ACCESS.2021.3139532

Comparing the Performance of C_{pk} and $\bar{X}$ Control Charts With the Generalized Multiple Dependent State Sampling Supplementary Signaling Rule

BRUNA S. COSTA AND ANTÔNIO F. B. COSTA
Institute of Production Engineering and Management, Federal University of Itajubá, Itajubá 37500-903, Brazil

Corresponding author: Bruna S. Costa (bsc.unifei@gmail.com)

The work of Antônio F. B. Costa was supported by the National Council for Scientific and Technological Development - CNPq (GRANT # 305133/2020-9).

ABSTRACT The C_{pk} index was originally created to measure the ability of the processes to produce products meeting specifications but, more recently, Rao and team proposed the use of the C_{pk} index to control processes. In reality, they investigated the performance of the C_{pk} chart with the GMDS (Generalized Multiple Dependent State Sampling) supplementary signaling rule. With the GMDS supplementary run rule, the C_{pk} chart signals when a point falls in the action region or when a point falls in the warning region after a sequence of m points, with less than k, in the central region. The points on the C_{pk} chart are the estimated values of the C_{pk} index obtained with the mean and the variance of the samples. Rao and team obtained the *ARLs* of the GMDS C_{pk} chart by simulation; reminding the *ARL* is the average number of samples the chart requires to signal a change in the process. This present work uses the Markov chain approach to obtain the *ARLs*, once this approach leads to exact results. The main conclusion is that the GMDS $\bar{X}$ chart is not only simpler to use than the GMDS C_{pk} chart, but it is also more sensitive to process changes.

INDEX TERMS Control charts, generalized multiple dependent state sampling, process capability index.

I. INTRODUCTION

Control charts are monitoring tools specially designed to detect changes in the process parameters. In general, the control charts have lower and upper control limits (*LCL* and *UCL*) and require the withdrawal of samples from the process. The values of the monitoring statistic, obtained with the sample observations, generate the charting points and, according to the standard signaling rule, if one of them falls beyond the control limits, then the control chart triggers an alarm [1].

In recent studies, the C_{pk} index has been used as the monitoring statistic of the control chart, that is, at each sampling point the C_{pk} index is calculated with the sample mean and standard deviation as the estimates of mean and standard deviation of the process. These sample values of the C_{pk} index are the charting points of the C_{pk} chart. For instance, Rao *et al.* [2] proposed the use of the C_{pk} chart with the GMDS (Generalized Multiple Dependent State Sampling) supplementary signaling rule, that means the C_{pk} chart signals when a point falls in the action region or, yet, when a point falling in the warning region is preceded by a sequence of m points with less than k in the central region. If $k = m$, the GMDS reduces to the MDS (Multiple Dependent State Sampling) [3]–[6]. The multiple dependent state sampling has also been used in combination with repetitive sampling, MDSRS [7]–[14].

So, supplementary run rules enhance the sensitivity of the control charts in signaling process shifts. It is possible to observe three recent articles focusing on the use of supplementary signaling rules [15]–[17].

Control charts based on capability index are drawing researchers' attention. Reference [18] proposed the use of the C_{pk} chart with the repetitive sampling scheme, that is, three different decisions are taken according to the sample point position; if the point falls outside (inside) the outer (inner)

The associate editor coordinating the review of this manuscript and approving it for publication was Giambattista Gruosso.

control limits, the process is declared out of control (in control). Alternatively, a point falling outside the inner control limits, but not outside the outer control limits, leads to the withdrawal of a new sample, then, the information of this new sample is used to decide the state of the process or to postpone the decision to the next sample. Reference [19] proposed the two-stage sampling, with the use of the *np*chart during the first stage and the C_{pk} chart during the second stage. Reference [20] considered the charting points as the estimated values of the C_{pk} index obtained with the median and the variance values of the samples. Reference [21] considered the charting points as the estimated values of the C_{pk} index obtained with the Gini's mean difference. Other capability indices have also been used to control processes [22]–[26].

Thus, the aim of this paper is to compare the performance of the C_{pk} and $\bar{X}$ charts, when the standard signaling rule of a single point in the action region is used in combination with the GMDS supplementary run rule. Therefore, section 2 presents the C_{pk} and $\bar{X}$ charts with the GMDS supplementary signaling rule. Section 3 describes the Markov Chains approach with which the exact *ARLs* and steady-states *ARLs* of the GMDS charts are computed. In Section 4, the *ARLs* of the two GMDS charts, C_{pk} and $\bar{X}$, are compared. In Section 5, the comparisons are based on their *SSARLs*. Section 6 displays a real example. Finally, section 7 brings some conclusions.

II. THE C_{pk} AND $\bar{X}$ CHARTS WITH GMDS SUPPLEMENTARY RUN RULE

The control chart proposed by Rao *et al.* [2] combines the use of the process capability index, as the monitoring statistic, with the generalized multiple dependent state sampling, as the supplementary signaling rule. The monitoring statistic of the C_{pk} chart is the C_{pk} index in (1):

$$\hat{C}_{pk} = min\left\{\frac{USL - \bar{X}}{3S}, \frac{\bar{X} - LSL}{3S}\right\} \tag{1}$$

Obtained with the mean and the standard deviation of the sample, respectively (2) and (3):

$$\bar{X} = (1/n)\sum_{i=1}^{n} X_i \tag{2}$$

$$S^2 = \sum_{i=1}^{n}\left(X_i - \bar{X}\right)^2/(n-1) \tag{3}$$

where n is the size of the samples.

In (2), the *USL* and the *LSL* are, respectively, the upper and the lower specification limits. The C_{pk} and the $\bar{X}$ charts with the GMDS supplementary run rule have inner (LCL_2, UCL_2) and outer (LCL_1, UCL_1) control limits shown in (4)-(7):

$$LCL_1 = E(MS) - k_1\sqrt{Var(MS)} \tag{4}$$

$$UCL_1 = E(MS) + k_1\sqrt{Var(MS)} \tag{5}$$

$$LCL_2 = E(MS) - k_2\sqrt{Var(MS)} \tag{6}$$

$$UCL_2 = E(MS) + k_2\sqrt{Var(MS)} \tag{7}$$

In (4)-(7), the *MS* is the monitoring statistic of the chart; if the chart is the C_{pk} chart, then $E(MS) = E\left(\hat{C}_{pk}\right)$ and $Var(MS) = Var\left(\hat{C}_{pk}\right)$. Alternatively, if the chart is the $\bar{X}$ chart, then $E(MS) = E\left(\bar{X}\right) = \mu_0$ and $Var(MS) = Var\left(\bar{X}\right) = \sigma^2/n$, where μ_0 and σ^2 are the in-control mean and variance of the process.

The opening parameters k_1 and k_2 are adjusted to meet the required ARL_0 - average number of samples between false alarms; it has been adopted an ARL_0 of 370.4. Rao *et al.* [2] obtained k_1 and k_2 by simulation, and they also used simulation to obtain the ARL_1 - average number of samples the chart requires to signal process mean increases (or decreases). The increase or decrease is expressed in units of σ and represented by δ; if μ_1 is the out-of-control mean, then (8):

$$\mu_1 = \mu_0 \pm \delta\sigma \tag{8}$$

Without losing generality, adopting $\mu_0 = 0$ and $\sigma = 1$.

It was also considered the symmetric case where $LSL = -USL$. The process is declared to be in control when (9):

$$LCL_2 \leq MS \leq UCL_2 \tag{9}$$

And out of control when (10) or (11):

$$MS > UCL_1 \tag{10}$$

$$MS < LCL_1 \tag{11}$$

If the current monitoring statistic point falls in the warning region (12) or (13):

$$LCL_1 \leq MS \leq LCL_2 \tag{12}$$

$$UCL_2 \leq MS \leq UCL_1 \tag{13}$$

Then the state of the process is decided by the previous m points: if less than k are in the central region (in between LCL_2 and UCL_2), then the process is declared to be out of control; otherwise, the process is declared to be in control.

III. THE MARKOV CHAIN TO OBTAIN THE EXPRESSION OF THE STEADY-STATE ARL

The work developed by Rao *et al.* [2] calculated the *ARLs* using simulation. Since it was not displayed some required inputs to run the simulation, such as $E(MS)$ and $Var(MS)$, it was not possible to recalculate the *ARLs*. As an alternative, it was used the Markov chains approach, that leads to exact *ARLs* and steady-state *ARLs* of the GMDS charts; reminding the steady-state *ARL* (*SSARL*) is the average number of samples the chart requires to signal a change in the process, under the assumption that until the monitoring statistic reaches its stationary distribution the process mean (μ) remains unaltered, with $\mu = \mu_0$.

The number of states with which the Markov chain is built is a function of m and k. To illustrate, let $m = k = 3$, then the states are defined by the position of the last four sample points. Fig. 1 presents the Markov chain with the states defined by the sequence (a, b, c, d), in which a, b, and c are the sample points positions of the third, second and first points before the last one, and d is the position of the last sample point; for instance (C, W, C, A) means the last

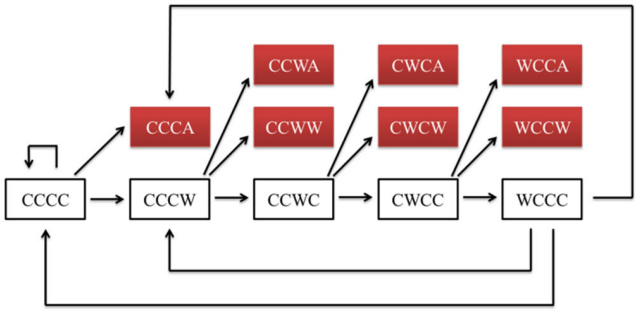

FIGURE 1. The Markov chains with states defined by the sequence (*a, b, c, d*).

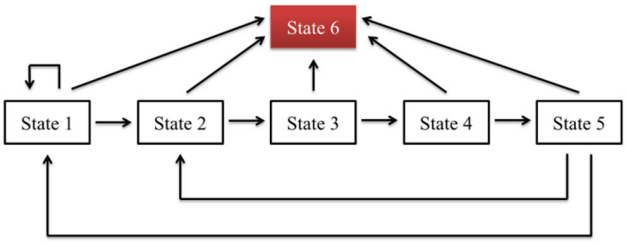

FIGURE 2. The Markov chains with five transient states and one absorbing state.

point is in the action region (represented by A), and the third, second and first points before the last one are, respectively, in the central (represented by C), in the warning (represented by W) and in the central regions. Fig. 2 shows that, if $m = k = 3$, then the Markov chain can be represented by five transient states (in white) and one absorbing state (in red).

Using the arrows of Fig. 1 as guide, the transition probability matrix is given by (14):

$$\boldsymbol{P} = \begin{pmatrix} p_{11} & p_{12} & 0 & 0 & 0 & p_{16} \\ 0 & 0 & p_{23} & 0 & 0 & p_{26} \\ 0 & 0 & 0 & p_{34} & 0 & p_{36} \\ 0 & 0 & 0 & 0 & p_{45} & p_{46} \\ p_{51} & p_{52} & 0 & 0 & 0 & p_{56} \\ 0 & 0 & 0 & 0 & 0 & 1 \end{pmatrix} = \begin{pmatrix} p_1 & p_2 & 0 & 0 & 0 & p_3 \\ 0 & 0 & p_1 & 0 & 0 & 1-p_1 \\ 0 & 0 & 0 & p_1 & 0 & 1-p_1 \\ 0 & 0 & 0 & 0 & p_1 & 1-p_1 \\ p_1 & p_2 & 0 & 0 & 0 & p_3 \\ 0 & 0 & 0 & 0 & 0 & 1 \end{pmatrix} \quad (14)$$

where p_{ij} denotes the transition probability in which i is the prior state and j is the current state. So:

- $p_1 = p_{11} = p_{23} = p_{34} = p_{45} = p_{51} = Pr\,[LCL_2 \leq MS \leq UCL_2]$;
- $p_2 = p_{12} = p_{52} = Pr\,[LCL_1 \leq MS \leq LCL_2] + Pr\,[UCL_2 \leq MS \leq UCL_1]$;
- $p_3 = p_{16} = p_{56} = Pr\,[MS > UCL_1] + Pr\,[MS < LCL_1]$;
- $p_{26} = 1 - p_{23}$;
- $p_{36} = 1 - p_{34}$;
- $p_{46} = 1 - p_{45}$.

Reference [27] displays that the first step to obtain the steady-state *ARL* is the construction of the matrix (**I-Q**), in which **I** is the 5 by 5 identity matrix and **Q** is the transition matrix given in (14), with the last row and column removed as displayed in (15):

$$(\boldsymbol{I} - \boldsymbol{Q}) = \begin{bmatrix} 1-p_1 & -p_2 & 0 & 0 & 0 \\ 0 & 1 & -p_1 & 0 & 0 \\ 0 & 0 & 1 & -p_1 & 0 \\ 0 & 0 & 0 & 1 & -p_1 \\ -p_1 & -p_2 & 0 & 0 & 1 \end{bmatrix} \quad (15)$$

The steady-state *ARL* is given by $\mathrm{S}'(\mathbf{I}\text{-}\mathbf{Q})^{-1}$, in which S is the vector with the stationary probabilities of being in each transient state. The inverse of (**I-Q**) is described in (16), as shown at the bottom of the next page.

Reference [27] presents that the vector S is the solution of $\mathrm{S}' = \mathbf{P}^*\mathrm{S}$, in which $\mathbf{P}^*$ is the transition probability matrix **P** with the absorbing state 6 transformed into a return to the state 1; in other words, after a false alarm the monitoring always returns to state 1 (the return to state 1 is equivalent to assume that the last four sample points are in the central region). Matrix $\mathbf{P}^*$ is shown in (17):

$$\boldsymbol{P}^* = \begin{bmatrix} p_1 + p_3 & p_2 & 0 & 0 & 0 \\ 1-p_1 & 0 & p_1 & 0 & 0 \\ 1-p_1 & 0 & 0 & p_1 & 0 \\ 1-p_1 & 0 & 0 & 0 & p_1 \\ p_1 + p_3 & p_2 & 0 & 0 & 0 \end{bmatrix} \quad (17)$$

The solution of $\mathrm{S}' = \mathbf{P}^*\mathrm{S}$ is given by (18):

$$S' = \begin{pmatrix} 1 - p_1^3 p_2 & p_2 & p_1 p_2 & p_1^2 p_2 & p_1^3 p_2 \end{pmatrix} / a \quad (18)$$

In which a is calculated through (19):

$$a = \left(1 + p_2 + p_1 p_2 + p_1^2 p_2\right) \quad (19)$$

Consequently, the steady-state *ARL* of the GMDS $\bar{X}$ chart is computed with the $\mathrm{S}'(\mathbf{I}\text{-}\mathbf{Q})^{-1}$ expression. The *ARL* of the GMDS $\bar{X}$ chart is also computed with the $\mathrm{S}'(\mathbf{I}\text{-}\mathbf{Q})^{-1}$ expression, but now with the first element of vector S being equal to one, and all the other elements being equal to zero.

IV. COMPARING THE ARLs OF THE GMDS $\bar{X}$ AND C_{pk} CHARTS

Table 1 presents the *ARL*s of the GMDS $\bar{X}$ chart given by $\mathrm{S}'(\mathbf{I}\text{-}\mathbf{Q})^{-1}$ with S'= (1,0…0) and also the *ARL*s of the GMDS C_{pk} chart published by Rao *et al.* [2].

The results show that depending on the (m, k) combination one chart is better than the other (the winning chart is in bold). For instance, if $(m, k) = (3,2)$ the GMDS C_{pk} chart is more sensitive than the $\bar{X}$ chart, but with $(m, k) = (4,2)$ the charts alter their positions: now the GMDS $\bar{X}$ chart is more sensitive than the GMDS C_{pk} chart. If $(m, k) = (3,3)$ or $(4,4)$, the GMDS C_{pk} chart signals faster small shifts ($\delta \leq 0.67$), but for larger shifts ($\delta \geq 0.89$), the GMDS $\bar{X}$ chart signals faster.

TABLE 1. The *ARLs* of the GMDS $\bar{X}$ and C_{pk} charts for $n = 5$.

	(m, k)		(3,3)		(3,2)		(4,4)		(4,3)		(4,2)	
			C_{pk}	$\bar{X}$	C_{pk}	$\bar{X}$	C_{pk}	$\bar{X}$	C_{pk}	$\bar{X}$	C_{pk}	$\bar{X}$
$\delta\sqrt{n}$	δ	k_1	5.5707	3.1000	5.7263	3.1000	5.6231	3.1000	5.3922	3.1000	5.3922	3.1000
		k_2	3.8828	2.3568	1.7355	1.8193	4.3735	2.4017	3.2858	1.9125	3.2858	1.5183
							ARLs					
0.5	0.22		**100.46**	141.33	**62.17**	140.73	**112.38**	140.51	97.84	138.00	95.65	141.26
1	0.45		**34.16**	34.18	**11.39**	32.29	**42.44**	33.90	32.38	**31.01**	32.03	**31.88**
1.5	0.67		**13.91**	10.90	**3.47**	10.03	**18.80**	10.90	11.92	**9.72**	11.19	**9.92**
2	0.89		6.72	**4.79**	**1.75**	4.55	9.54	**4.83**	5.06	**4.51**	4.88	**4.66**
2.5	1.12		3.83	**2.72**	**1.25**	2.72	5.50	**2.75**	2.68	**2.73**	2.10	**2.86**
3	1.34		2.52	**1.85**	**1.09**	1.91	3.56	**1.86**	1.77	**1.91**	1.58	**1.99**

In terms of overall performance, the GMDS C_{pk} chart with $(m, k) = (3,2)$ is the winner of all control charts under comparison. The authors were not able to verify the simulated *ARL*s obtained by Rao *et al.* [2] because it was not provided all the required inputs to run the simulations, that is, *E(MS)*, *Var (MS)* and *USL* values. As an alternative, it was decided to investigate the properties of the GMDS C_{pk} chart by using the $S'(I\text{-}Q)^{-1}$ expression. In the next section, it will be compared the *SSARL*s of the GMDS C_{pk} chart with the *SSARL*s of the GMDS $\bar{X}$ chart; both *SSARL*s were obtained by using $S'(I\text{-}Q)^{-1}$ expression.

V. COMPARING SSARLs OF THE GMDS $\bar{X}$ AND C_{pk} CHARTS

In order to obtain the cumulative distribution of the $\hat{C}_{pk}$ statistic it was used the recent result presented by Costa [28] that evidenced (20):

$$\Pr\left[\hat{C}_{pk} < C_o\right] = \int_0^\infty Pr[\sqrt{n}\,(3sC_o - LSL - \mu)\,/\sigma < Z < \sqrt{n}\,(USL - 3sC_o - \mu)\,/\sigma]f\,(s)\,ds \quad (20)$$

In (20), $Z \sim N(0,1)$ and $f(s)$ is the density function of the sample standard deviation given by (21):

$$f\,(s) = \frac{2}{\sigma}\sqrt{\frac{(n-1)^{n-1}}{2}}\left(\frac{s}{\sigma}\right)^{n-2}\left\{\frac{exp[-0.5(n-1)\,(s/\sigma)^2}{\Gamma[0.5\,(n-1)]}\right\} \quad (21)$$

The density function of the $\hat{C}_{pk}$ statistic is totally asymmetric; Fig. 3 shows the case for which $n = 5$ and

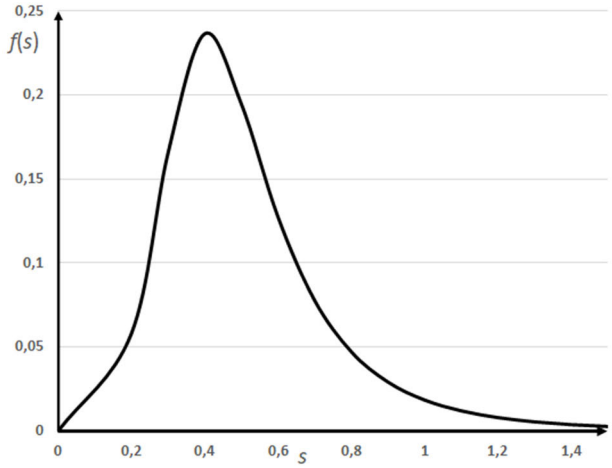

FIGURE 3. The asymmetric density function $f(s)$ of the $\hat{C}_{pk}$.

$USL = 1.5$. Based on that, it was chosen to use symmetric warning and action limits regarding the in-control probabilities (a, b), in which (a) is the probabilities to obtain a $\hat{C}_{pk}$ point in the action region and (b) is the probabilities to obtain a $\hat{C}_{pk}$ point in the warning region. If $LCL_1 = ka_1$ (in which *ka* indicates the opening parameter for action region), $LCL_2 = kw_1$ (in which *kw* indicates the opening parameter for warning region), $UCL_2 = kw_2$ and $UCL_1 = ka_2$, it is possible to calculate (22)-(24):

$$Pr[\hat{C}_{pk} < ka_1 =] = a/2 \quad (22)$$

$$(\boldsymbol{I} - \boldsymbol{Q})^{-1} = \frac{1}{1 - p_1 - p_1^3 p_2}\begin{bmatrix} 1 - p_1^3 p_2 & p2 & p_1 p_2 & p_1^2 p_2 & p_1^3 p_2 \\ p_1^4 & 1 - p_1 & p_1 - p_1^2 & p_1^2 - p_1^3 & p_1^3 - p_1^4 \\ p_1^3 & p_1^2 p_2 & 1 - p_1 & p_1 - p_1^2 & p_1^2 - p_1^3 \\ p_1^2 & p_1 p_2 & p_1^2 p_2 & 1 - p_1 & p_1 - p_1^2 \\ p1 & p2 & p_1 p_2 & p_1^2 p_2 & 1 - p_1 \end{bmatrix} \quad (16)$$

TABLE 2. The *SSARLs* of the GMDS $\bar{X}$ and C_{pk} charts for n = 5.

(m, k)		(3,3)		(3,2)		(4,4)		(4,3)		(4,2)	
		C_{pk}	$\bar{X}$	C_{pk}	$\bar{X}$	C_{pk}	$\bar{X}$	C_{pk}	$\bar{X}$	C_{pk}	$\bar{X}$
δ	ka_2	2.7164	k_1=3.1000	2.7164	3.1000	2.7164	3.10	2.7164	3.1000	2.7164	3.1000
	kw_2	1.5182	k_2=2.3577	1.061647	1.8204	1.568	2.4028	0.8866	1.9137	0.8866	1.5196
	kw_1	0.1060		0.1699		0.1005		0.1589		0.2055	
	ka_1	0.0085		0.00851		0.0085		0.0085		0.0085	
		SSARLs									
0.25		176.86	118.93	180.18	117.94	175.84	118.15	177.37	115.25	182.81	118.29
0.5		44.23	25.33	45.53	23.64	43.7	25.15	43.75	22.7	47.01	23.27
0.75		12.67	7.87	12.94	7.29	12.57	7.9	12.41	7.12	13.47	7.28
1		5.01	3.57	5.13	3.48	5.02	3.61	5.02	3.48	5.37	3.62
1.25		2.65	2.12	2.74	2.18	2.67	2.15	2.73	2.19	2.86	2.29
1.5		1.73	1.52	1.79	1.57	1.74	1.52	1.79	1.57	1.84	1.61

$$Pr[\hat{C}_{pk} > ka_2] = a/2 \tag{23}$$

$$Pr[kw_1 < \hat{C}_{pk} < kw_2] = 1 - a - b \tag{24}$$

Consequently, the probabilities p_1, p_2 and p_3 with which the transition probability matrix **P** is built and used to obtain the *SSARL*s of the GMDS C_{pk} chart are given by (25)-(27):

$$p_1 = Pr\left[k_{w1} \leq \hat{C}_{pk} \leq k_{w2}\right] \tag{25}$$

$$p_3 = Pr\left[\hat{C}_{pk} > k_{a2}\right] + Pr\left[\hat{C}_{pk} < k_{a1}\right] \tag{26}$$

$$p_2 = 1 - p_1 - p_3 \tag{27}$$

Table 2 presents the *SSARL*s of the GMDS $\bar{X}$ chart ($n = 5$) and the *SSARL*s of the GMDSC_{pk} chart ($n = 5$, $UCL = 1.5$); the GMDS C_{pk} chart reaches its best overall performance with $UCL = 1.5$.

The results show the superiority of the GMDS $\bar{X}$ chart; that is, regardless of the (m, k) combination, the *SSARL*s values of the GMDS $\bar{X}$ chart are always the lower ones. It is worthy to note that all *SSARL*s values were checked by simulation. Table 2 also reveals the following observations:

a) In terms of charts performance, the signaling rules $(m, k) = (3, 3)$ and $(m, k) = (4, 4)$ are practically equivalent;
b) Comparing the signaling rules $(m, k) = (3, 3)$ and $(m, k) = (3, 2)$, or yet, the rules $(m, k) = (4, 4)$ and $(m, k) = (4, 3)$, the second signaling rule always reduces the ability of the C_{pk} chart to detect mean increases or decreases, and slightly improves the ability of the $\bar{X}$ chart in signaling moderate or small mean increases or decreases ($\delta \leq 1$);
c) Comparing the signaling rules $(m, k) = (4, 3)$ and $(m, k) = (4, 2)$, the second one reduces the ability of the C_{pk} and the $\bar{X}$ charts to detect mean increases or decreases.

VI. REAL EXAMPLE

Suppose that a company, which supplies shafts, is facing considerable losses due to the production of defective items.

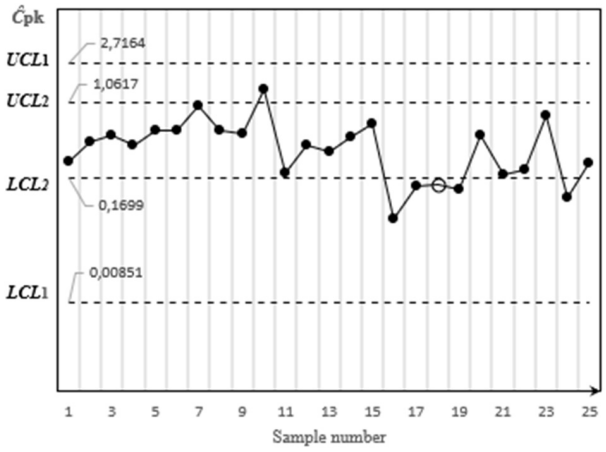

FIGURE 4. The GMDS $\hat{C}_{pk}$ chart for the real example.

The diameter of the shafts has been the cause of rejection. As the specifications are very tight, a minor shift in the process mean leads to manufacturing the shafts with diameters beyond the specifications; so, the shift should be detected as fast as possible. Past data shows the standard deviation (σ) of the diameters is pretty close to 0.0010 inches. This example was originally explored by Costa and Rahim [29].

Table 3 presents the diameter X of 25 samples with 5 shafts each; the data of the first 15 samples were simulated with the process mean free of shifts, whereas the data of the last 10 samples were simulated with an increased process mean of one standard deviation. Fig. 4 and fig. 5 present, respectively, the C_{pk} and the $\bar{X}$ charts with the GMDS supplementary run rule $(m, k) = (3, 2)$; in both charts, the eighteenth sample signals the mean shift. The C_{pk} chart signals with the eighteenth sample because the sixteenth and seventeenth samples are in-between the LCL_1 and LCL_2 lower limits. On the other hand, the $\bar{X}$ chart signals with the eighteenth sample because the sixteenth and seventeenth samples are in-between the UCL_2 and UCL_1 upper limits.

As a result, both the C_{pk} and the $\bar{X}$ charts are considered practical tools for process surveillance subject to moderate

TABLE 3. The X_s, $\bar{X}$ and $\hat{C}_{pk}$ values for the real example.

#	X_1	X_2	X_3	X_4	X_5	$\bar{X}$	$\hat{C}_{pk}$
1	0.7472	0.7500	0.7506	0.7503	0.7496	0.7496	0.2564
2	0.7514	0.7500	0.7509	0.7511	0.7500	0.7507	0.4133
3	0.7488	0.7512	0.7509	0.7502	0.7498	0.7502	0.4754
4	0.7497	0.7514	0.7488	0.7509	0.7508	0.7503	0.3818
5	0.7490	0.7488	0.7503	0.7502	0.7496	0.7496	0.5448
6	0.7498	0.7496	0.7503	0.7494	0.7485	0.7495	0.5285
7	0.7494	0.7498	0.7501	0.7507	0.7501	0.7500	0.9673
8	0.7488	0.7501	0.7509	0.7491	0.7503	0.7498	0.5337
9	0.7502	0.7515	0.7487	0.7500	0.7498	0.7500	0.4947
10	0.7495	0.7501	0.7504	0.7498	0.7499	0.7500	1.4422
11	0.7496	0.7492	0.7499	0.7484	0.7479	0.7490	0.1918
12	0.7510	0.7516	0.7493	0.7485	0.7493	0.7499	0.3716
13	0.7508	0.7481	0.7516	0.7496	0.7491	0.7498	0.3183
14	0.7511	0.7505	0.7496	0.7502	0.7514	0.7506	0.4498
15	0.7506	0.7503	0.7502	0.7501	0.7486	0.7500	0.6218
16	0.7512	0.7509	0.7503	0.7533	0.7507	0.7513	0.0638
17	0.7520	0.7508	0.7513	0.7502	0.7517	0.7512	0.1387
18	0.7516	0.7513	0.7517	0.7494	0.7515	0.7511	0.1474
19	0.7498	0.7513	0.7499	0.7523	0.7520	0.7511	0.1296
20	0.7498	0.7508	0.7508	0.7497	0.7484	0.7499	0.4803
21	0.7519	0.7510	0.7513	0.7512	0.7484	0.7507	0.1833
22	0.7490	0.7511	0.7498	0.7513	0.7522	0.7507	0.2048
23	0.7494	0.7500	0.7505	0.7502	0.7509	0.7502	0.7541
24	0.7504	0.7518	0.7491	0.7510	0.7529	0.7511	0.1046
25	0.7517	0.7515	0.7495	0.7513	0.7497	0.7507	0.2388

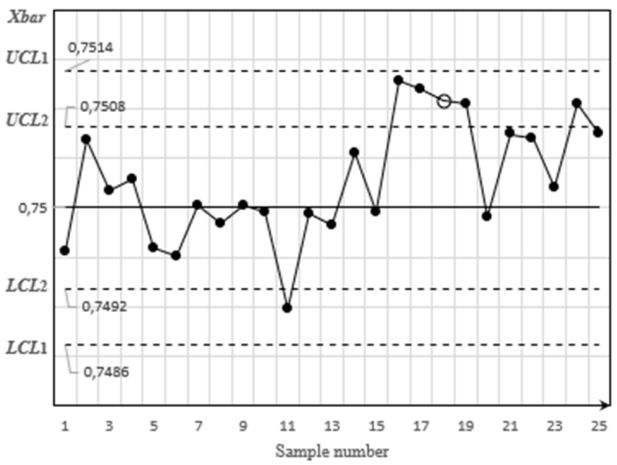

FIGURE 5. The GMDS $\bar{X}$ chart for the real example.

disturbances. Depending on the parameters, one chart can be perceived as more efficient than the other one. In this real example, both charts displayed the same performance for the supplementary run rule $(m, k) = (3, 2)$.

VII. CONCLUSION

Thanks to the Markov chains properties, it was obtained the exact expression of the *SSARLs*. To illustrate how exact expressions of the *SSARLs* can be obtained by the Markov chain approach, it was considered the control chart with the GMDS supplementary run rule $(m, k) = (3, 3)$. It is important to notice that this expression is independent of the statistic in use to control the process.

Inspired by the work proposed by Rao *et al.* [2] in which the authors investigate the performance of the C_{pk} control chart with the supplementary run rule GMDS, this article broadens the investigation to also include the $\bar{X}$ control chart with GMDS run rule. Consequently, the *ARL* and *SSARL* values calculated demonstrate insightful analysis on the comparison of the performance of GMDS C_{pk} and $\bar{X}$ control charts.

In terms of comparison, it was proved that the GMDS C_{pk} chart should be considered with care, because it is pretty slow in signaling mean shifts. The GMDS $\bar{X}$ chart with the supplementary run rule $(m, k) = (4, 3)$ has the best overall performance.

It is worthy to note that, when the monitoring statistic of the control chart is the $\hat{C}_{pk}$, that is, the C_{pk} index obtained with the $\bar{X}$ and S sample values, the specification limits can no longer be seen as the limits beyond which a product is considered defective. In fact, they are now tuning parameters of the control chart because they deeply affect the speed in which the C_{pk} chart signals. The GMDS C_{pk} chart reaches its best overall performance with $UCL = 1.5$.

REFERENCES

[1] D. C. Montgomery, *Introduction to Statistical Process Control*, 8th ed. Hoboken, NJ, USA: Wiley, 2019.

[2] G. Srinivasa Rao, M. A. Raza, M. Aslam, A. H. Al-Marshadi, and C.-H. Jun, "A variable control chart based on process capability index under generalized multiple dependent state sampling," *IEEE Access*, vol. 7, pp. 34031–34044, 2019.

[3] M. Aslam, R. A. R. Bantan, and N. Khan, "Design of X-bar control chart using multiple dependent state sampling under indeterminacy environment," *IEEE Access*, vol. 7, pp. 152233–152242, 2019.

[4] M. Albassam and M. Aslam, "Monitoring non-conforming products using multiple dependent state sampling under indeterminacy–An application to juice industry," *IEEE Access*, vol. 8, pp. 172379–172386, 2020.

[5] A. I. Shawky, M. Aslam, and K. Khan, "Multiple dependent state sampling-based chart using belief statistic under neutrosophic statistics," *J. Math.*, vol. 2020, pp. 1–14, Aug. 2020.

[6] Q. Wan, "Economic-statistical design of integrated model of VSI control chart and maintenance incorporating multiple dependent state sampling," *IEEE Access*, vol. 8, pp. 87609–87620, 2020.

[7] M. S. Aldosari, M. Aslam, and C.-H. Jun, "A new attribute control chart using multiple dependent state repetitive sampling," *IEEE Access*, vol. 5, pp. 6192–6197, 2017.

[8] M. S. Aldosari, M. Aslam, N. Khan, L. Ahmad, and C.-H. Jun, "A new S^2 control chart using multiple dependent state repetitive sampling," *IEEE Access*, vol. 6, pp. 49224–49236, 2018.

[9] M. Aslam, "Attribute control chart using the repetitive sampling under neutrosophic system," *IEEE Access*, vol. 7, pp. 15367–15374, 2019.

[10] M. Aslam, "Control chart for variance using repetitive sampling under neutrosophic statistical interval system," *IEEE Access*, vol. 7, pp. 25253–25262, 2019.

[11] A. Loganathan and M. Gunasekaran, "Design of multiple dependent state repetitive group sampling plans based on exponentiated exponential distribution," *J. Test. Eval.*, vol. 49, no. 2, pp. 1315–1325, 2021.

[12] M. Aslam, S. Balamurali, P. Jeyadurga, and M. A. Raza, "Monitoring number of non-conforming items based on multiple dependent state repetitive sampling under truncated life tests," *Commun. Statist.-Theory Methods*, Nov. 2020, doi: 10.1080/03610926.2020.1847294.

[13] M. Aslam, A. Shafqat, G. S. Rao, J.-C. Malela-Majika, and S. C. Shongwe, "Multiple dependent state repetitive sampling-based control chart for Birnbaum–Saunders distribution," *J. Math.*, vol. 2020, Oct. 2020, Art. no. 8539361.

[14] M. Aslam, C.-H. Yen, C.-H. Chang, A. H. Al-Marshadi, and C.-H. Jun, "A multiple dependent state repetitive sampling plan based on performance index for lifetime data with type II censoring," *IEEE Access*, vol. 7, pp. 49377–49391, 2019.

[15] O. A. Adeoti and J.-C. Malela-Majika, "Double exponentially weighted moving average control chart with supplementary runs-rules," *Qual. Technol. Quant. Manage.*, vol. 17, no. 2, pp. 149–172, Mar. 2020.

[16] J. Oh and C. H. Weiß, "On the individuals chart with supplementary runs rules under serial dependence," *Methodol. Comput. Appl. Probab.*, vol. 22, no. 3, pp. 1257–1273, Sep. 2020.

[17] A. Yeganeh and A. Shadman, "Monitoring linear profiles using artificial neural networks with run rules," *Expert Syst. Appl.*, vol. 168, Apr. 2021, Art. no. 114237.

[18] L. Ahamad, M. Aslam, and C.-H. Jun, "The design of a new repetitive sampling control chart based on process capability index," *Trans. Inst. Meas. Control*, vol. 38, no. 8, pp. 971–980, 2015.

[19] M. Aslam, N. Khan, L. Ahmad, C.-H. Jun, and J. Hussain, "A mixed control chart using process capability index," *Sequential Anal.*, vol. 36, no. 2, pp. 278–289, Apr. 2017.

[20] M. Aslam, G. Rao, A. Al-Marshadi, L. Ahmad, and C.-H. Jun, "Control charts for monitoring process capability index using median absolute deviation for some popular distributions," *Processes*, vol. 7, no. 5, p. 287, May 2019.

[21] M. Aslam, G. S. Rao, L. Ahmad, and C.-H. Jun, "A new control chart using GINI C_{PK}," *Commun. Statist.-Theory Methods*, Apr. 2020, doi: 10.1080/03610926.2020.1746971.

[22] M. Morita, I. Arizono, I. Nakase, and I. Takemoto, "Economical operation of the C_{pm} control chart for monitoring process capability index," *Int. J. Adv. Manuf. Technol.*, vol. 43, pp. 304–311, Sep. 2009.

[23] M. T. Carot, A. Sagbas, and J. M. Sanz, "A new approach for measurement of the efficiency of C_{pm} and C_{pmk} control charts," *Int. J. Qual. Res.*, vol. 7, no. 4, pp. 605–622, 2013.

[24] M. Aslam, M. Mohsin, and C.-H. Jun, "A new T-chart using process capability index," *Commun. Statist.-Simul. Comput.*, vol. 46, no. 7, pp. 5141–5150, Aug. 2017.

[25] J. Xu and C. Peng, "Parametric bootstrap process capability index control charts for both mean and dispersion," *Commun. Statist.-Simul. Comput.*, vol. 48, no. 10, pp. 2936–2954, Nov. 2019.

[26] D. S. Wang and H. Y. T. Y. Yang Koo, "A new approach for measurement of the efficiency of C_{pm} and C_{pmk} control charts," *Int. J. Ind. Syst. Eng.*, vol. 36, pp. 32–48, Feb. 2020.

[27] E. Cinlar, *Introduction to stochastic processes*, 1st ed. New York, NY, USA: Dover, 1975.

[28] A. F. B. Costa, "The performance of the C_{pk} chart," *Commun. Statist.-Simul. Comput.*, Sep. 2021, doi: 10.1080/03610918.2021.1949471.

[29] A. F. B. Costa and M. A. Rahim, "Joint X bar and R charts with two stage samplings," *Qual. Rel. Eng. Int.*, vol. 20, pp. 699–708, Jul. 2004.

BRUNA S. COSTA received the M.S. degree in production engineering from the Federal University of Itajubá, Brazil, in 2019, where she is currently pursuing the Ph.D. degree in production engineering, researching in process monitoring field.

ANTÔNIO F. B. COSTA currently teaches statistics with the Federal University of Itajubá, Brazil. He has published around 100 articles, most of them dealing with the monitoring of processes.